

Contract No:

This document was prepared in conjunction with work accomplished under Contract No. DE-AC09-08SR22470 with the U.S. Department of Energy.

Disclaimer:

This work was prepared under an agreement with and funded by the U.S. Government. Neither the U. S. Government or its employees, nor any of its contractors, subcontractors or their employees, makes any express or implied: 1. warranty or assumes any legal liability for the accuracy, completeness, or for the use or results of such use of any information, product, or process disclosed; or 2. representation that such use or results of such use would not infringe privately owned rights; or 3. endorsement or recommendation of any specifically identified commercial product, process, or service. Any views and opinions of authors expressed in this work do not necessarily state or reflect those of the United States Government, or its contractors, or subcontractors.

Impact of Noble Metals and Mercury on Hydrogen Generation during High Level Waste Pretreatment at the Savannah River Site

D.C. Koopman

T. B. Edwards

M.E. Stone

Savannah River National Laboratory, Aiken, SC 29808

The Defense Waste Processing Facility (DWPF) at the Savannah River Site vitrifies radioactive High Level Waste (HLW) for repository internment. The process consists of three major steps: waste pretreatment, vitrification, and canister decontamination/sealing. HLW consists of insoluble metal hydroxides (primarily iron, aluminum, calcium, magnesium, manganese, and uranium) and soluble sodium salts (carbonate, hydroxide, nitrite, nitrate, and sulfate). The pretreatment process in the Chemical Processing Cell (CPC) consists of two process tanks, the Sludge Receipt and Adjustment Tank (SRAT) and the Slurry Mix Evaporator (SME) as well as a melter feed tank. During SRAT processing, nitric and formic acids are added to the sludge to lower pH, destroy nitrite and carbonate ions, and reduce mercury and manganese. During the SME cycle, glass formers are added, and the batch is concentrated to the final solids target prior to vitrification. During these processes, hydrogen can be produced by catalytic decomposition of excess formic acid. The waste contains silver, palladium, rhodium, ruthenium, and mercury, but silver and palladium have been shown to be insignificant factors in catalytic hydrogen generation during the DWPF process.

A full factorial experimental design was developed to ensure that the existence of statistically significant two-way interactions could be determined without confounding of the main effects with the two-way interaction effects. Rh ranged from 0.0026-0.013% and Ru ranged from 0.010-0.050% in the dried sludge solids, while initial Hg ranged from 0.5-2.5 wt%, as shown in Table 1. The nominal matrix design consisted of twelve SRAT cycles. Testing included: a three factor (Rh, Ru, and Hg) study at two levels per factor (eight runs), three duplicate midpoint runs, and one additional replicate run to assess reproducibility away from the midpoint. Midpoint testing was used to identify potential quadratic effects from the three factors. A single sludge simulant was used for all tests and was spiked with the required amount of noble metals immediately prior to performing the test. Acid addition was kept effectively constant except to compensate for variations in the starting mercury concentration. SME cycles were also performed during six of the tests.

Table 1. Test Matrix for Simulations

Run	Position	Rh, wt%	Ru, wt%	Hg, wt%
RhRuHg1	L-L-L	0.00263	0.01012	0.506
RhRuHg12	H-L-L	0.01315	0.01012	0.506
RhRuHg10	L-H-L	0.00263	0.05056	0.505
RhRuHg14	H-H-L	0.01314	0.05054	0.505
RhRuHg5	L-L-H	0.00257	0.00990	2.475
RhRuHg6	H-L-H	0.01287	0.00990	2.474
RhRuHg7	L-H-H	0.00257	0.04948	2.472
RhRuHg8	H-H-H	0.01285	0.04946	2.472
RhRuHg9	M-M-M	0.00780	0.03000	1.500
RhRuHg11	M-M-M	0.00780	0.03000	1.500
RhRuHg15	M-M-M	0.00780	0.03000	1.500
RhRuHg13	H-L-H	0.01287	0.00990	2.474

An average composition based on nine independent samples of the simulant prior to the Rh-Ru-Hg matrix study is given in Table 2 for the elements after calcining at 1100°C. These were determined by inductively coupled plasma-atomic emission spectroscopy (ICP-AES).

Table 2. Wt% Calcined Elemental Composition of Sludge

	ABC Blend Simulant wt%
Al	16.0
Ba	0.21
Ca	2.50
Cr	0.15
Cu	0.10
Fe	21.5
K	0.19
Mg	1.5
Mn	3.9
Na	12.7
Ni	0.87
Pb	0.047
Si	1.62
Ti	0.019
Zn	0.20
Zr	0.44

Table 3 gives corresponding density and solids data. The wt% total solids were measured on the slurry. The wt% dissolved solids were measured on the

filtered supernate (no insoluble solids). These two measured values were used to calculate the wt% soluble and insoluble solids of the slurry.

Table 3. Density and Solids Data on Blend Simulant

	ABC Blend Simulant
Wt% total solids	22.8
Wt% insoluble solids	16.8
Wt% soluble solids	6.0
Wt% calcined solids	16.0
Slurry Density, g/mL	1.175
Supernate Density, g/mL	1.053

Table 4 summarizes the available information on total anions in the simulant slurry. Values are mg indicated species per kg of the untrimmed simulant slurry. Results come from a variety of analytical and computational methods. Ion chromatography (IC) is the preferred analytical method, but some species which were added to the simulant fell below the instrument detection limits. Anions, such as oxide, phosphate, and oxalate, are not necessarily present as dissociated species.

Table 4. Anion Data on Blend Simulant Slurry

ABC Blend Simulant	mg/kg
OH ⁻ (by ion-mass balance)	80,000
NO ₂ ⁻	17,950
NO ₃ ⁻	13,790
O ²⁻ (by ion-mass balance)	13,000
C ₂ O ₄ ²⁻ (by recipe calculation)	1,400
PO ₄ ³⁻ (by ICP P)	160
SO ₄ ²⁻ (by IC)	1,625
SO ₄ ²⁻ (by ICP S)	1,350
Total Inorganic Carbon	1350
Cl ⁻	390
F ⁻ (by recipe calculation)	47

Nominal scaled DWPF SRAT/SME processing conditions were generally used; however, neither cycle had a heel from a prior batch.

- The SRAT air purge scaled to 230 scfm in DWPF.
- A 200 ppm antifoam addition was made prior to nitric acid addition.
- A 100 ppm antifoam addition was made prior to formic acid addition.
- Nitric and formic acid addition were at 93°C.
- Acid was scaled based on two gallons per minute for a 6,000 gallons batch size (DWPF scale).

- A 500 ppm antifoam addition was made prior to going to boiling following acid addition.
- Boiling targeted the scaled 5,000 lbs/hr at DWPF scale.
- SRAT dewatering typically took about 50 minutes.
- Reflux followed dewatering. The end of the 12-hour reflux period defined the end of the SRAT cycle.
- After SRAT product samples were pulled, the air purge was adjusted to the scaled SME rate, 74 scfm.
- A 100 ppm antifoam addition was made at the start of the SME.
- Two canister decon water additions were performed at the scaled equivalent of 1,000 gallons water per canister decon and were boiled off.
- Two frit-water-formic acid slurry additions (50% frit with formic acid at 1.5 g of 90 wt% acid/100 g frit) targeting 35% sludge oxides followed the final canister decon dewatering.
- After the second frit-water-formic acid slurry addition, the SME was dewatered to 50 wt% total solids.

A complete SRAT/SME simulation took about 36 hours measured from the start of heating prior to acid addition in the SRAT until the time that the SME product had cooled to less than 50°C. Simulations were run continuously except for a short break between the SRAT and SME cycles.

Agilent 3000A micro GC's were used on all twelve runs. Column-A can collect data related to He, H₂, O₂, N₂, NO, and CO, while column-B can collect data related to CO₂ and N₂O. GC's were calibrated with a standard gas containing 0.499 vol% He, 1.010 vol% H₂, 20.00 vol% O₂, 51.0 vol% N₂, 25.0 vol% CO₂ and 2.50 vol% N₂O. Room air was used to give a two point calibration for N₂. The GC's were checked with calibration gas following the SRAT cycle and again following the SME cycle. NO vol% data were obtained semi-quantitatively using the historical ratios of He/NO area factors for the individual GC's, since no calibration gas with NO was available. No evidence for CO generation was obtained while examining the region of the chromatogram where it would elute.

Experimental Results

Impact of Rhodium

Rhodium causes a sharp peak in the hydrogen generation rate following acid addition as shown in Figure 1. The height of the peak was affected by rhodium, but not ruthenium or mercury. (At the 90% confidence level.) Notation: H-L-H stands for high Rh, low Ru, and high Hg.

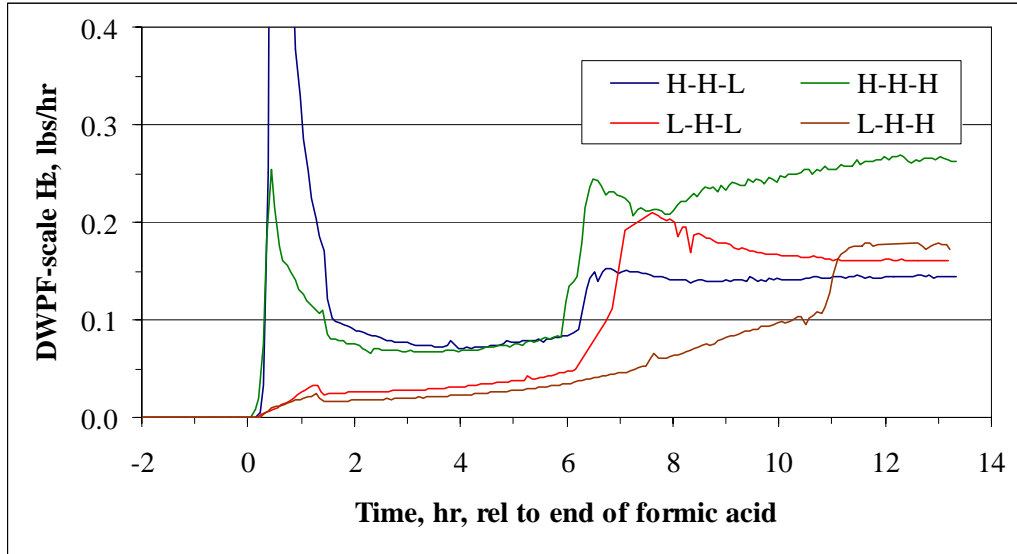


Figure 1. Rhodium Concentration Impact on Catalytic Hydrogen Generation

Impact of Ruthenium

In contrast to the immediate sharp peak noted with rhodium, hydrogen generation from ruthenium slowly builds during the run and does not decay, as shown in Figure 2. The height of the peak is affected by ruthenium concentration as well as formic acid amount. Rhodium concentration can also have a significant impact by reducing the amount of formic acid remaining when the reactions involving ruthenium start.

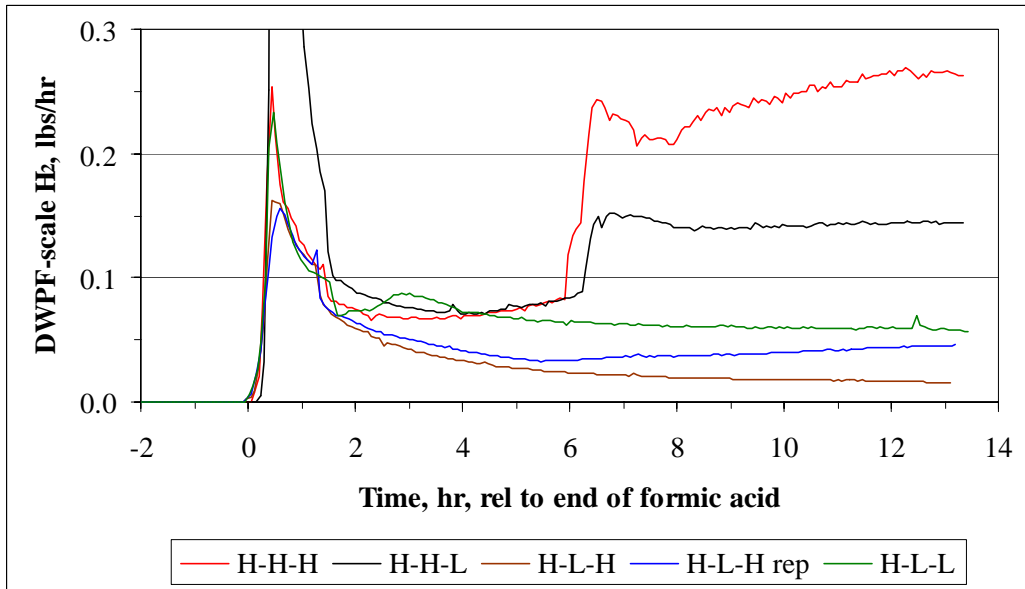


Figure 2. Ruthenium Concentration Impact on Catalytic Hydrogen Generation

Impact of Mercury

The impact of mercury is shown in Figure 3 and is typical of result pairs with constant Rh-Ru and varying Hg. Hydrogen generation was qualitatively affected by variations in mercury, but the effect was not significant during statistical modeling using JMP software.

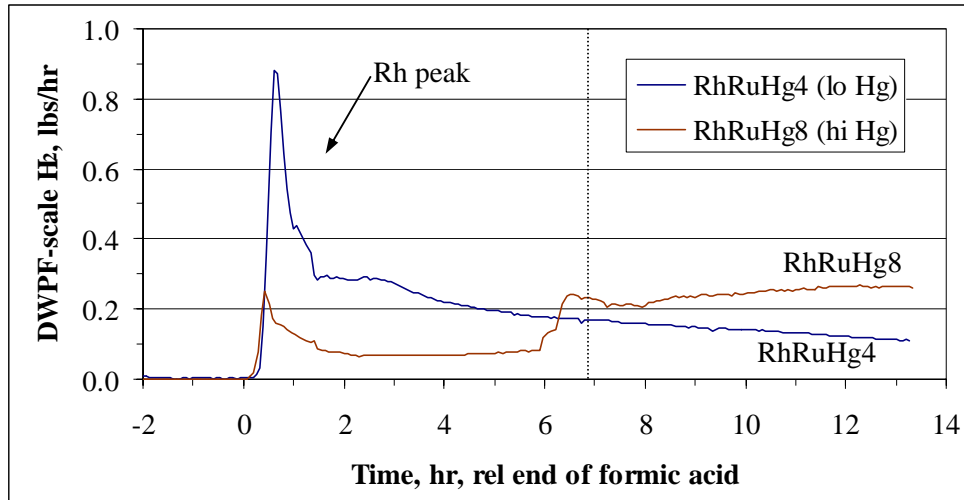


Figure 3. Mercury Concentration Impact on Catalytic Hydrogen Generation

SME Cycle Results

In general, the hydrogen generation rate in the SME cycle was controlled by the amount of formic acid remaining at the end of the SME cycle and ruthenium concentration. The primary impact of rhodium and mercury concentration was their impact on the amount of formic acid destruction during the SRAT cycle.

Statistical Results

Response measures, such as the maximum hydrogen generation rate during the SRAT cycle, were created from the SRAT processing data in order to evaluate the statistical significance of various responses due to changes in the three matrix factors. Five distinct response measures were created for hydrogen production during the SRAT cycle, as shown in Table 5. These were:

- Total mass of hydrogen produced, g
- SRAT overall maximum (peak) hydrogen generation rate, DWPF-scale lbs/hr
- Maximum hydrogen generation rate in the first two hours after acid addition, lbs/hr
- Maximum hydrogen generation rate in the last four hours of reflux, lbs/hr
- Time of the maximum hydrogen generation rate, in decimal hours

Table 5. Process Measures for SRAT Hydrogen

	Overall peak H ₂ , lbs/hr	Total H ₂ , g	Overall H ₂ Peak Time, hr	0-2 hr H ₂ peak, lbs/hr	9-13 hr H ₂ peak, lbs/hr
Low Mercury Runs					
RhRuHg1	0.0596	0.0199	13.22	0.0180	0.0596
RhRuHg12	0.2330	0.0493	0.47	0.2330	0.0612
RhRuHg10	0.2103	0.0681	7.62	0.0330	0.1785
RhRuHg14	1.415	0.1028	0.53	1.415	0.1459
High Mercury Runs					
RhRuHg5	0.0317	0.0136	13.24	0.0220	0.0317
RhRuHg6	0.1624	0.0239	0.43	0.1624	0.0186
RhRuHg7	0.1793	0.0451	12.54	0.0249	0.1793
RhRuHg8	0.2687	0.1167	12.28	0.2534	0.2687
Midpoint Mercury Runs					
RhRuHg9	0.1118	0.0346	0.87	0.1118	0.0712
RhRuHg11	0.0866	0.0228	0.67	0.0866	0.0448
RhRuHg15	0.1356	0.0375	12.07	0.0730	0.1356
RhRuHg13 [§]	0.1552	0.0333	0.60	0.1552	0.0456

§ - this was a replicate trial matched to RhRuHg6 conditions

Fitting considered eight potential model terms. These were Rh, Ru, Hg, the three pair-wise interactions, the single ternary interaction, and a generic quadratic term. The total hydrogen produced during the SRAT cycle will be used to illustrate the general modeling procedure followed for all process measures. The modeling procedure relied on the stepwise regression platform in JMP statistical analysis software (version 5.0.1). Table 6 indicates the terms that appeared in the regression model (75% confidence to enter and 90% to remain) using a capital P for terms with positive coefficients and a capital N for terms with negative coefficients. Dashes indicate terms that did not enter the model.

Table 6. Model for Total Hydrogen Generated

Rh	Ru	Hg	Rh*Ru	Rh*Hg	Ru*Hg	Quad	R ²	LoF
P	P	N	P	-	-	P	0.95	N

The first three columns indicate whether or not Rh, Ru, or Hg had a statistically significant main effect (in this case all three did). The next three columns indicate whether there were significant interactions between terms (in this case, one between Rh and Ru). The next column indicates if a quadratic effect (non-linear effect due to one or more individual variables) was significant. In this case, there was a significant quadratic, or non-linear, impact on total hydrogen mass. The next to last column gives the R² value of the model

(recognize that a four term model has five constant coefficients; when there are only 12 results to fit, R^2 tends to be fairly large). Finally, the last column indicates whether or not “lack of fit”, or LoF, was indicated (N = no lack of fit, and Y = lack of fit). No lack of fit was the desired outcome of the model fitting process.

The preferred quadratic factor was Hg^2 for the total hydrogen mass response model. The presence of Hg^2 forced the model to bring in the linear Hg factor, which otherwise would not have been a statistically significant factor at the 90% confidence level. Selecting either Rh^2 or Ru^2 as the quadratic term caused a small reduction in R^2 because both Hg and Hg^2 left the model. Consequently, the primary factors controlling the total mass of hydrogen produced during the SRAT cycle were modeled to be Rh , Ru and their pair-wise interaction along with a possible small contribution from Hg and/or a quadratic effect.

The positive coefficient on the Rh - Ru interaction indicated that the low-low and high-high cases tended to be enhanced in total hydrogen mass while the mixed high-low cases tended to be inhibited in total hydrogen. This suggests an optimum Rh/Ru ratio for hydrogen generation exists somewhere in the neighborhood of the fission yield ratio (low-low and high-high cases of Rh - Ru were at the theoretical fission yield ratio).

The statistical model predictions are compared to the twelve total hydrogen mass values in Figure 4, taken from the JMP software.

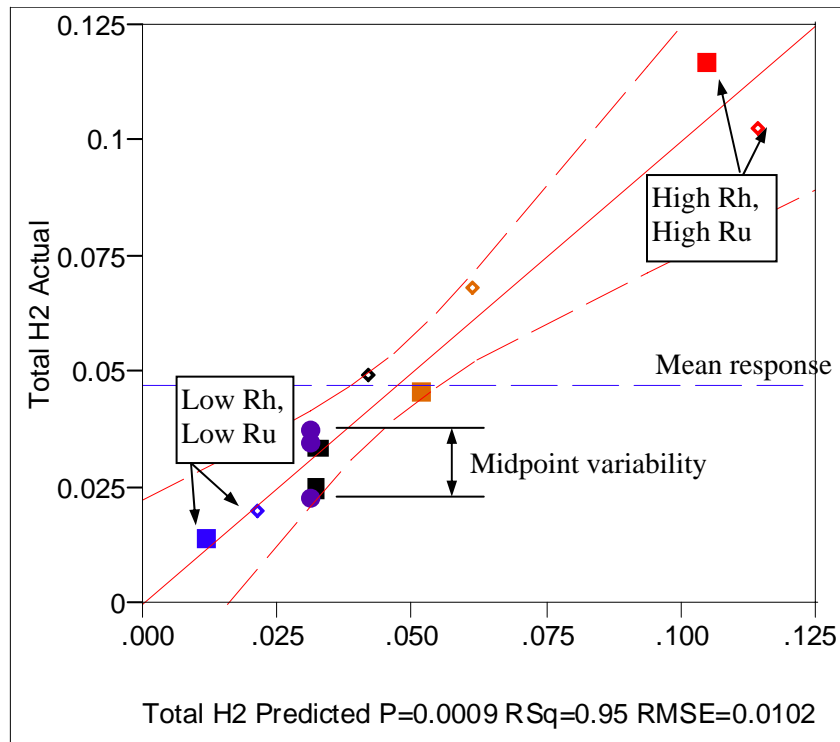


Figure 4. Example comparison of model and data

Data are spread along the model line (45° line) with some small amount of scatter, and with all of the points lying inside the dashed confidence interval curves (no evidence of outliers). Note that the variability in reproducing the midpoint case (solid circles) is comparable to the width of the confidence interval curves about the 45° line. Variability due to lack of reproducibility is not explained by linear statistical models based on the controlled factors.

Results from each of the other process measures is shown in Table 7.

Table 7. Statistical Regression Results

Measure	Rh	Ru	Hg	Rh*Ru	Rh*Hg	Ru*Hg	Qua d	R ²	LoF
Peak H ₂	(P)	P	-	-	-	-	-	0.42	Y
0-2hr Peak H ₂	P	-	-	-	-	-	-	0.25	N
9-13hr Peak H ₂	-	P	-	-	-	-	-	0.74	N
SRAT Peak time	N	-	-	-	-	-	-	0.41	N

The statistical regression confirmed the qualitative analysis that rhodium is responsible for the initial hydrogen peak, ruthenium is responsible for the second peak and the either could be responsible for the highest peak. Rhodium also controlled the timing of the peak (early or late). Mercury may inhibit the initial peak from rhodium, but that could leave more formic acid to react with ruthenium and increase the overall peak, so no significant correlation was noted between peak hydrogen and mercury concentration.

Findings from this study were:

- Rh controlled the maximum hydrogen generation rate in the first two hours after acid addition.
- Ru controlled the maximum hydrogen generation rate after the period of Rh control had passed, typically 6-8 hours later.
- Increasing the ratio of Hg/Rh shifted the time of the maximum hydrogen generation rate from the earlier Rh period to the later Ru period when holding Ru at its fission yield ratio to Rh.
- A previously documented inhibiting effect of Hg on hydrogen generation apparently requires very little mercury in terms of moles Hg/mole Rh (or Ru). Additional increases in Hg concentration produce only a minimal inhibition in hydrogen generation rates.
- Low Hg runs do not necessarily bound high Hg runs for the maximum hydrogen generation rate over the full CPC cycle. Two of the four Rh-Ru combinations had a cross-over point where the hydrogen generation rate

- in the high Hg run went from always lower to always higher than in the low Hg run.
- Maximum hydrogen generation rates in the high Hg runs could exceed the maximum hydrogen generation rates from the low Hg runs.

References

1. Koopman, D. C., 2008, "Catalytic Interactions of Rhodium, Ruthenium, and Mercury during Simulated DWPF CPC Processing with Hydrogen Generation", WSRC-STI-2008-00235, Savannah River Nuclear Solutions, Aiken, SC.
2. Koopman, D. C. and Edwards, T. B., 2009, "Statistical Evaluation of Processing Data from the Ru-Ru-Hg Matrix Study", SRNL-STI-2008-00235, Savannah River Nuclear Solutions, Aiken, SC.